MULTI INPUT LUO CONVERTER BASED HYBRID ELECTRIC VEHICLE USING BLDC MOTOR

N.S.Pratheeba
Assistant Professor/EEE, Francis Xavier Engineering College, Tirunelveli.
pratheeba.ns@francisxavier.ac.in

A.Amala Manuela
Assistant Professor/EEE, Francis Xavier Engineering College, Tirunelveli.
amalamanuela.a@francisxavier.ac.in

A.Petchiammal
UG Student/EEE, Francis Xavier Engineering College, Tirunelveli
petchiammal.a@gmail.com

Abstract- Renewable energy sources have become a popular alternative electrical energy source where power generation in conventional ways is not practical. In the last few years the photovoltaic and wind power generation have been increased significantly. In this study, we proposed a hybrid energy system which combines both solar panel and wind turbine generator as an alternative for conventional source of electrical energy like thermal and hydro power generation. A simple control technique which is also cost effective has been proposed to track the operating point at which maximum power can be coerced from the PV system and wind turbine generator system under continuously changing environmental conditions. The LUO converter provides constant voltage to the voltage source inverter from hybrid energy. This voltage is given to the PMBLDC motor based vehicle. The Maximum power point tracking methods perturb and observe algorithm is used extract maximum power from the hybrid system. The entire hybrid system is described given along with comprehensive simulation results that discover the feasibility of the system. A software simulation model is developed in Matlab/Simulink and the hardware is developed using DSPIC30F2010 controller.

Keywords-LUO converter, PMBLDC Motor, Hybrid Energy system.

I. INTRODUCTION

In a PMBLDCM, the dc field winding of the rotor is replaced by a permanent magnet to produce the air-gap magnetic flux. Having the magnets on the rotor, electrical losses due to field winding of the machine get reduced and the lack of the field losses improves the thermal characteristics of the PM machines and its efficiency. Absence of mechanical components like brushes and slip rings makes the motor lighter, high power to weight ratio for which a higher efficiency and reliability is achieved

BLDC motor drives, systems in which a permanent magnet excited synchronous motor is fed with a variable frequency inverter controlled by a shaft position sensor. There appears a lack of commercial simulation packages for the design of controller for such BLDC motor drives. One main reason has been that the high software development cost incurred is not justified. For their typical low cost fractional/integral kW application areas such as NC machine tools and robot drives, even it could imply the possibility of demagnetizing the rotor magnets during commissioning or tuning stages. Nevertheless, recursive prototyping of both the motor and inverter may be involved in novel drive configurations for advance and specialized applications, resulting in high developmental cost of the drive system. Improved magnet material with high (B.H), product also helps push the BLDC motors market to tens of kW application areas where commissioning errors become prohibitively costly. Modeling is therefore essential and may offer potential cost savings.

II. EXISTING SYSTEM

A solar photovoltaic (SPV) powered brushless DC (BLDC) motor drive for water pumping is presented in this paper. The current sensors of BLDC motor and the voltage sensor at the DC bus of voltage source inverter (VSI) are eliminated completely. Instead, the speed is controlled by adjusting the DC bus voltage of VSI. The fundamental frequency switching pulses are generated to operate the VSI in order to

minimize the switching losses and to enhance the efficiency of proposed system. A DC-DC Cuk converter is utilized to operate the SPV array at its maximum power. The starting current of BLDC motor is bounded by an optimal initialization and selection of the control parameters, perturbation size and frequency while tracking the peak power of SPV array. The performance of proposed BLDC motor drive is thoroughly evaluated

and its potential is demonstrated under realistic operating conditions. The simulated results and an experimental validation along with a comprehensive comparison with the existing techniques demonstrate prominence of the proposed drive for SPV based water pumping.

2.1 CIRCUIT DIAGRAM

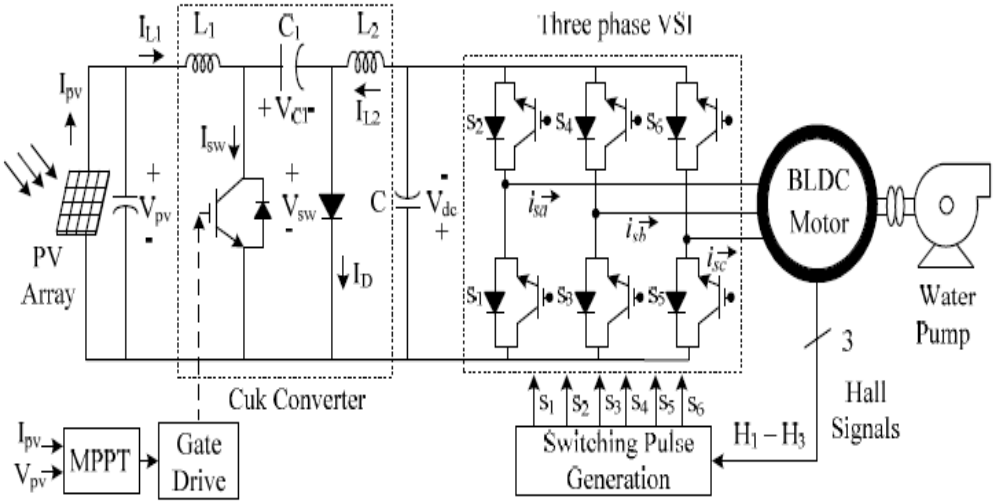

Figure 1: Existing system circuit diagram

2.2 OPERATION

A voltage follower approach is used for the control of the CUK converter operating in DICM. A single voltage sensor is required for controlling the dc link voltage for speed control of BLDC motor, and inherent MPPT is achieved at the Dc side. Fig. 1 shows a complete block diagram for the control of dc link voltage. This control scheme consists of a 'reference voltage generator,' a 'voltage error generator,' a voltage controller, and a PWM generator. A reference voltage generator generates a reference voltage V ∗ dc by multiplying the reference speed ω∗ with the motor's voltage constant kv as

$V^{*}dc = kv\omega$. (1)

The voltage error generator compares this reference dc link voltage (V ∗dc) with the sensed dc link voltage (Vdc) to generate an error voltage (Ve), which is given as

$Ve(k) = Vdc(k)^{*} - Vdc(k)$ (2)

where 'k' represents the kth sampling instance. This error voltage Ve is given to a voltage proportional–integral (PI) controller to generate a controlled output voltage Vcc, which is expressed as

$Vcc(k) = Vcc(k-1) + Kp\{Ve(k) - Ve(k-1)\} + KiVe(k)$ (3)

where Kp and Ki are the proportional and integral gains of the PI controller, respectively. Finally, the PWM signals are generated by comparing the output of PI controller (Vcc) with the high-frequency sawtooth signal (*md*), which are given as for

VS >0;_if *md* < *V*cc then *Sw*1 = 'ON' if *md* ≥ *V*cc then *Sw*1 = 'OFF'_for *VS* <0;_if m*d* < *V*cc then *Sw*2 = 'ON'if m*d* ≥ *V*cc then *Sw*2 = 'OFF'_(4) where *Sw*1 and *Sw*2 represent the gate signals to PFC switches *Sw*1 and *Sw*2, respectively Hall-effect position sensors are used to sense the rotor position to achieve electronic commutation of BLDC motor. A standard commutation technique is used for this trapezoidal back electromotive force (EMF) BLDC motor, where only two stator phases conduct at any given instant

of time. With the help of rotor position information, the switches in the VSI are switched ON and OFF to ensure proper direction of flow of current in respective windings. Hall-effect position sensors (*Ha*, *Hb*, and *Hc*) are used for sensing the rotor position on a span of 60◦ for electronic commutation. A line current *iab* is drawn from the dc link, whose magnitude depends on the applied dc link voltage *V*dc, back EMFs (*ean* and *ebn*), resistances (*Ra* and *Rb*), and mutual and self-inductances (*M* and *La* and *Lb*) of the stator windings.

2.3 EXISTING SYSTEM RESULTS

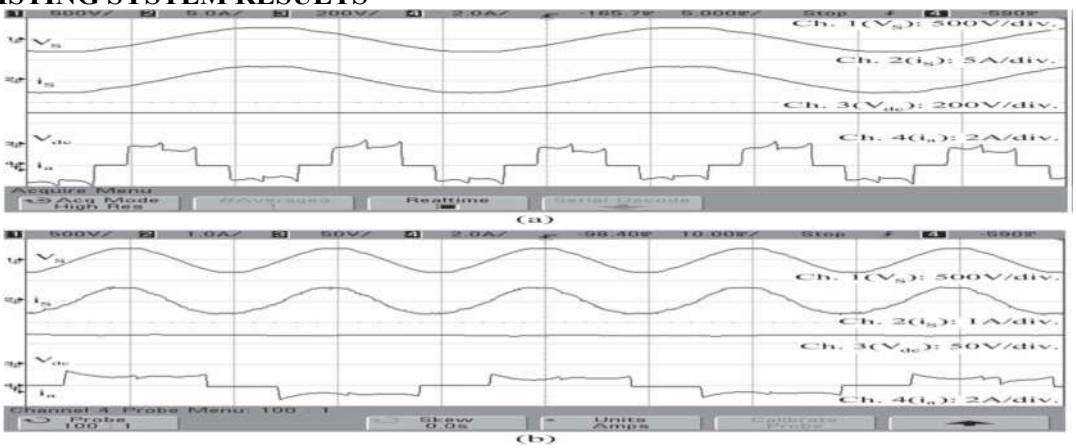

Figure. 2 Performance of the proposed drive at rated condition with supply voltage as 220 V and dc link voltage as (a) 310 V and (b) 70 V.

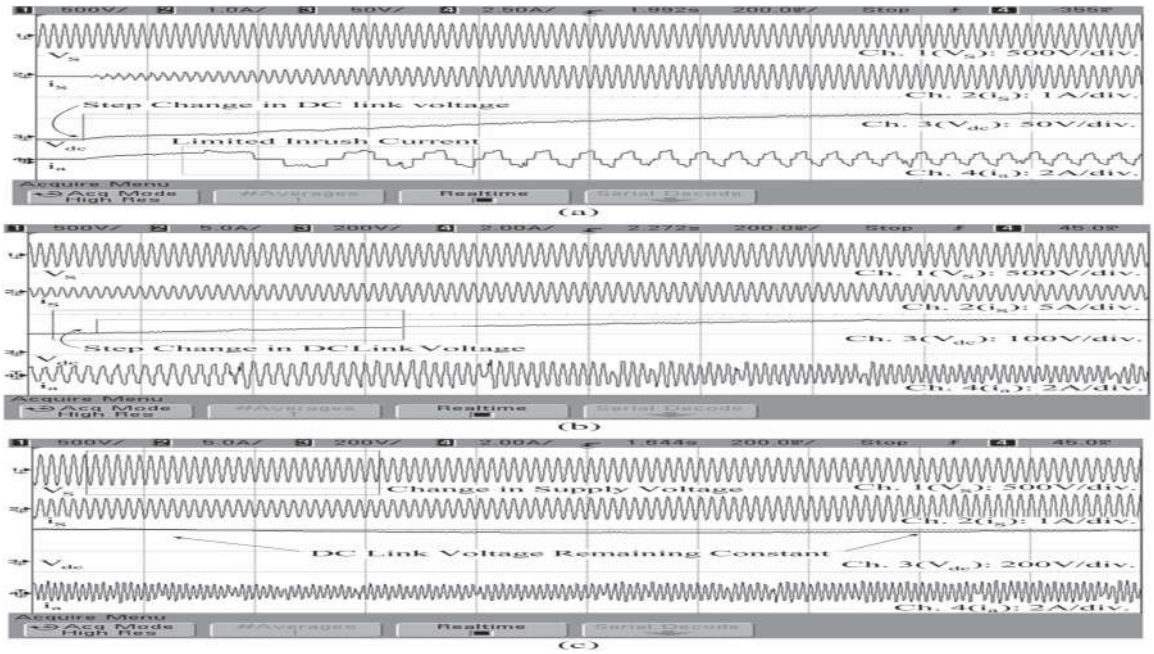

Figure 3 Existing system waveforms

DRAWBACKS

- High ripples in the Solar output voltage.
- Incremental conductance algorithm not provides constant DC voltage.
- CUK converter output voltage is inverted.
- Discontinuous input current waveform.

III. PROPOSED SYSTEM

A solar photovoltaic (SPV) powered brushless DC (BLDC) motor drive for water pumping is presented in this project. The current sensors of BLDC motor and the voltage sensor at the DC bus of voltage source inverter (VSI) are eliminated completely. Instead, the speed is controlled by adjusting the DC bus voltage of VSI. The fundamental frequency switching pulses are generated to operate the VSI in order to minimize the switching losses and to enhance the efficiency of proposed system. A DC-DC modified LUO converter is utilized to operate the SPV array at its maximum power. The starting current of BLDC motor is bounded by an optimal initialization and selection of the control parameters, perturbation size and frequency while tracking the peak power of SPV array.

The performance of proposed BLDC motor drive is thoroughly evaluated and its potential is demonstrated under realistic operating conditions. The simulated results and an experimental validation along with a comprehensive comparison with the existing techniques demonstrate prominence of the proposed drive for SPV based water pumping. The fuzzy logic based MPPT algorithm extracts maximum power from the solar panel. The PI controller is used to achieve the closed loop speed control operation.

3.1 BLOCK DIAGRAM

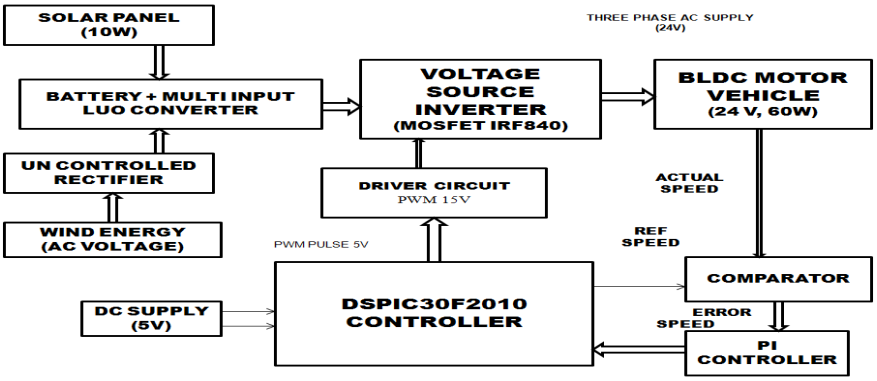

Figure 4 Proposed system block diagram

3.2 CIRCUIT DIAGRAM

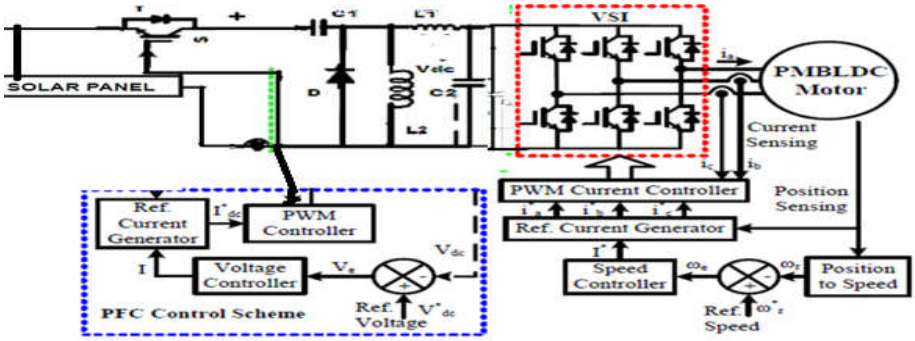

Figure 5 Proposed system circuit diagram

3.3 OPERATION

The proposed LUO converter is designed to operate in DICM such that current in inductors *Li*1 and *Li*2 becomes discontinuous for a switching period. Fig 5 shows different modes of operation during a complete switching period for positive and negative half-cycles of the supply voltage, respectively.

Mode I-A: As shown in Fig 5when switch *Sw*1 is turned on, the input side inductor *Li*1 starts charging via diode *Dp*, and current *iLi* increases, whereas the intermediate capacitor *C*1 starts discharging

via switch *Sw*1 to charge the dc link capacitor *Cd*. Therefore, the voltage across intermediate capacitor *VC*1 decreases, whereas the dc link voltage *V*dc increases.

Mode I-B: When switch *Sw*1 is turned off, the energy stored in inductor *Li*1 discharges to dc link capacitor *Cd* via diode *D*1, as shown in Fig 5. The current *iLi* reduces, whereas the dc link voltage continues to increase in this mode of operation.Intermediate capacitor *C*1 starts charging, and voltage *VC*1 increases.

Mode I-C: This mode is the DCM of operation as the current in input inductor *Li*1 becomes zero, as shown in Fig 5. The intermediate capacitor *C*1 continues to hold energy and retains its charge, whereas the dc link capacitor *Cd* supplies the required energy to the load. The similar behavior of the converter is realized for the other negative half-cycle of the supply voltage. An inductor *Li*2, an intermediate capacitor *C*2, and diodes *Dn* and *D*2 conduct in a similar way.

A voltage follower approach is used for the control of the LUO converter operating in DICM. A single voltage sensor is required for controlling the dc link voltage for speed control of BLDC motor, and inherent PFC is achieved at the ac mains . Fig. 4 shows a complete block diagram for the control of dc link voltage. This control scheme consists of a 'reference voltage generator,' a 'voltage error generator,' a voltage controller, and a PWM generator. Hall-effect position sensors are used to sense the rotor position to achieve electronic commutation of BLDC motor.

A standard commutation technique is used for this trapezoidal back electromotive force (EMF) BLDC motor, where only two stator phases conduct at any given instant of time. With the help of rotor position information, the switches in the VSI are switched ON and OFF to ensure proper direction of flow of current in respective windings. Hall-effect position sensors (*Ha*, *Hb*, and *Hc*) are used for sensing the rotor position on a span of 60◦ for electronic commutation. A line current *iab* is drawn from the dc link, whose magnitude depends on the applied dc link voltage *V*dc, back EMFs (*ean* and *ebn*), resistances (*Ra* and *Rb*), and mutual and self-inductances (*M* and *La* and *Lb*) of the stator windings. The comparator compares the actual and reference speed of the BLDC motor and the error signal is fed to the fuzzy logic controller, the fuzzy logic output is added with the PWM pulses, so that the motor will run at constant speed.

3.4 SIMULATION RESULTS

3.4.1 INPUT DC VOLTAGE WAVEFORM

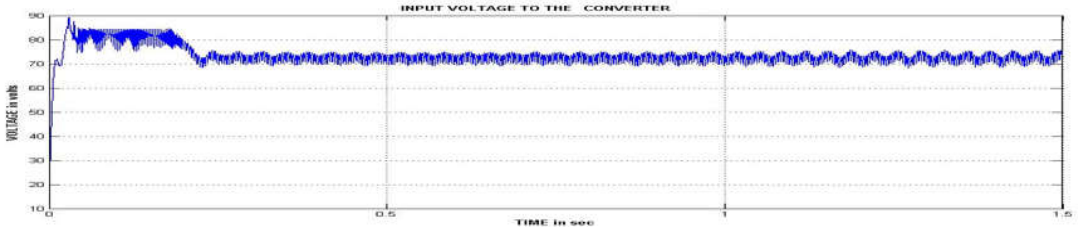

Figure 6 Input DC voltage waveform

The figure 6 shows the input DC voltage waveform which is produced from solar.

3.4.2 INPUT AC CURRENT WAVEFORM

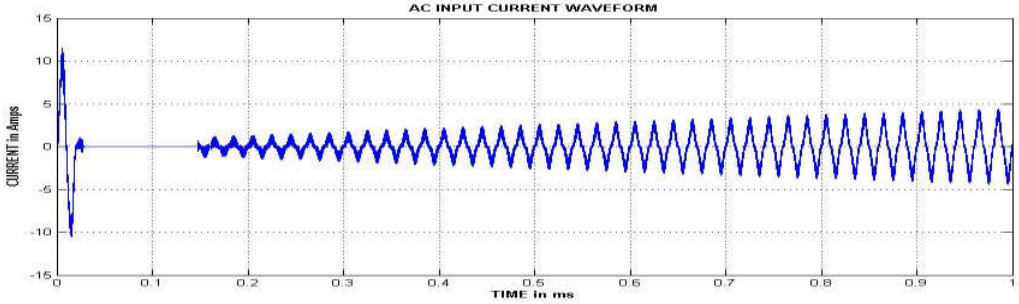

Figure 7 Input AC current waveform

The figure 7 shows input motor AC current waveform, which has affected by the BLDC motor back emf also its having harmonics.

3.4.3 PWM PULSE TO THE LUO CONVERTER SWITCH

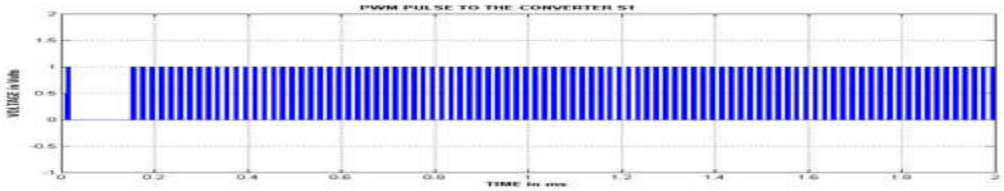

Figure 8 PWM pulse to the LUO converter switch

The figure 8 shows the PWM pulses which has produced by PWM generator and it is fed to the LUO converter switch.

3.4.5 LUO CONVERTER OUTPUT WAVEFORM

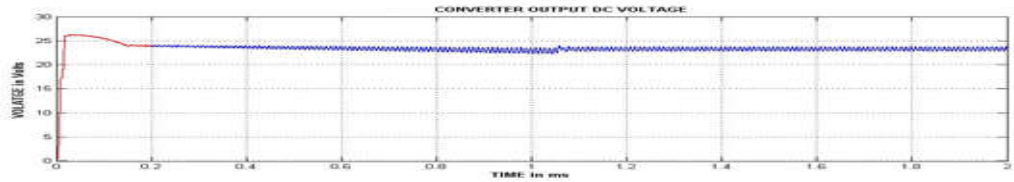

Figure 9 Output voltage of the LUO converter

The figure 9 shows the output voltage of the LUO converter , the maximum peak over shoot comes to settle at 0.015sec.

3.4.6 VOLTAGE SOURCE INVERTER OUTPUT VOLTAGE WAVEFORM

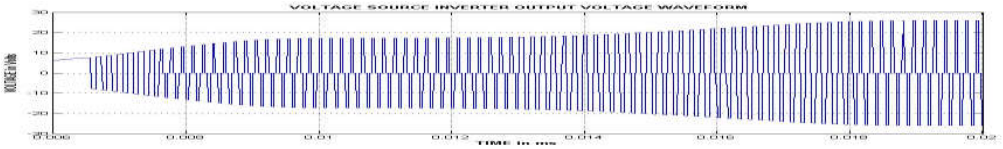

Figure 10 Voltage source inverter output voltage

The figure 10 shows the inverter output voltage with 24V amplitude it is given to the three phase BLDC motor.

3.4.7 BLDC MOTOR BACK EMF WAVEFORM

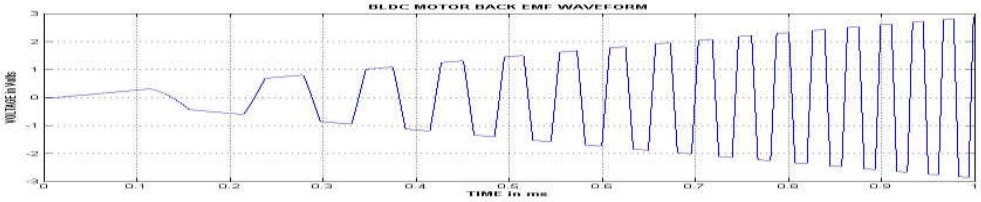

Figure 11 BLDC motor Back emf waveform

The figure 11 shows the BLDC motor back emf waveform due its 120 degree pole arc rotor construction.

3.4.8 BLDC MOTOR STATOR CURRENT WAVEFORM

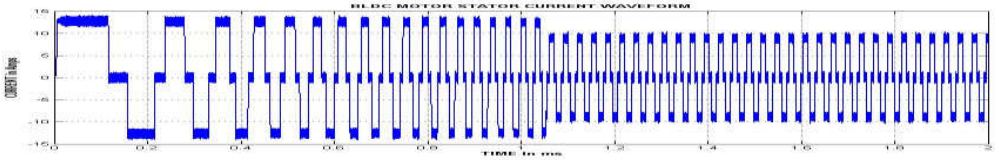

Figure 12 BLDC motor stator current waveform

The figure 12 shows the three phase BLDC motor stator current waveform, at starting the current is high like a Induction motor.

3.4.9 BLDC MOTOR SPEED WAVEFORM USING SPEED CONTROLLER

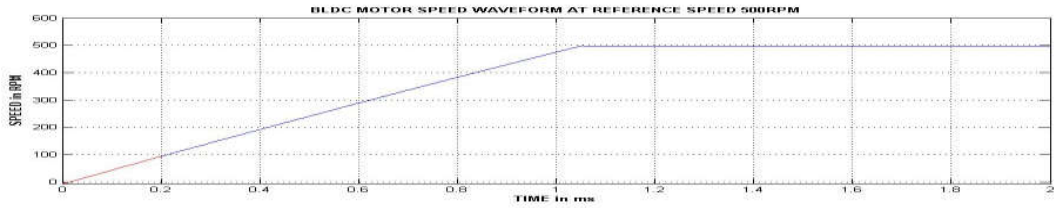

Figure 13 BLDC motor stator speed waveform using PI controller

The figure 13 shows the Speed waveform of the BLDC motor using PI based speed control.

IV. CONCLUSION

The proposed scheme has been validated through a demonstration of its various steady state, starting and dynamic performances. The performance of the system has been simulated using the MATLAB toolboxes. The DC link voltage and motor phase current sensing elements have been absolutely eliminated, resulting in a simple and cost-effective drive. The VSI has adopted a fundamental frequency switching, offering an enhanced efficiency due to the reduced switching losses in VSI. The other desired functions are speed control through variable DC link voltage without any additional circuit and a soft starting of the motor-pump. The LUO converter has provided an unbounded MPPT region and non-pulsating currents, eliminating the ripple filters. The detailed comparative analysis of the proposed and the existing work, have ultimately manifested the superiority of the proposed framework.

REFERENCES

1. Kenjo, T.; and Nagamori, S. (1985). *Permanent-magnet brushless DC motors*. Oxford University Press.
2. Sokira, T.J.; and Jaffe, W. (1989). *Brushless DC motors: Electronic Commutation and Control*. Tab Books USA.
3. Hendershort, J.R., Jr; and Miller, T.J.E. (1994). *Design of brushless permanent-magnet motors*. Oxford University Press, USA.
4. Gieras, J.F.; and Wing, M. (2002). *Permanent Magnet Motor Technology – Design and Application*. Marcel Dekker Inc., New York.
5. Pillay, P.; and Krishnan, R. (1989). Modeling, simulation and analysis of a permanent magnet brushless dc motor drives, part II: the brushless dc motor drive. *IEEE Trans. Ind. Appl.*, 25(2), 274-279.
6. International Standard IEC 61000-3-2, (2000). Limits for harmonic current emissions (Equipment input current ≤ 16 A per phase).
7. Brkovic, M.; and Cuk, S. (1992). Input current shaper using Cuk converter. *Proc. IEEE Telecommunications Energy Conference, 1992. INTELEC '92., 14th International*, 532 – 539.
8. Sebastian, J.; Cobos, J.A.; Lopera, J.M.; and Uceda, U. (1995). The determination of the boundaries between continuous and discontinuous conduction modes in PWM DC-to-DC converters used as power factor preregulators. *IEEE Trans. on Power Electronics*, 10(5), 574 – 582.
9. Tuckey, A.M.; and Patterson, D.J. (1996). The design and development of a high power factor current source controller for small appliance brushless DC motors. *Applied Power Electronics Conference and Exposition, 1996. APEC '96. Conference Proceedings 1996., Eleventh Annual*, 2, 778-781.
10. Simonetti, D.S.L.; Sebastian, J.; and Uceda, J. (1997). The discontinuous conduction mode Sepic and Cuk power factor preregulators: analysis and design. *IEEE Trans. Ind. Electron*., 44(5), 630 – 637.
11. Singh, B.; Singh, B.P.; and Kumar, M. (2003). PFC converter fed PMBLDC motor drive for air conditioning. *Institution of Engineers (India) Journal-EL*, 84, 22-27.
37th IEEE, 1-10. 12. Singh, B.; Murthy, S.S.; Singh, B.P.; and Kumar, M. (2003). Improved power quality converter fed permanent magnet AC motor for air conditioning. *Electric Power System Research*, 65(3), 239-245.
13. Gopalarathnam, T.; and Toliyat, H.A. (2003). A new topology for unipolar brushless dc motor drive with high power factor. *IEEE Trans. Power on Electronics*, 18(6), 1397-1404.

14. García, O.; Cobos, J.A.; Prieto, R.; Alou, P.; and Uceda, J. (2003). Single phase power factor correction: A survey. *IEEE Trans. Power on Electronics*, 18(3), 749-755.
15. Barkley, A.; Michaud, D.; Santi, E.; Monti, A.; and Patterson, D. (2006). Single stage brushless DC motor drive with high input power factor for single phase applications. *Power Electronics Specialists Conference, 2006. PESC '06.*